Neurosci Bull June 1, 2011, 27(3): 143–155. http://www.neurosci.cn
DOI: 10.1007/s12264-011-1028-2

·Original Article·

Combined administration of *D*-galactose and aluminium induces Alzheimer-like lesions in brain

Fei XIAO[1,*], Xiao-Guang LI[2,3,*], Xiao-Yu ZHANG[1], Jun-Dai HOU[1], Lian-Feng LIN[1], Qin GAO[2,3], Huan-Min LUO[1,2,3]

[1]*Department of Pharmacology, School of Medicine, Jinan University, Guangzhou 510632, China*
[2]*Institute of Brain Science, Jinan University, Guangzhou 510632, China*
[3]*Joint Laboratory for Brain Function and Health, Jinan University and The University of Hong Kong, Jinan University, Guangzhou 510632, China*

Abstract: Objective It has been reported that *D*-galactose (*D*-gal) can model subacute aging, and aluminum (Al) acts as a neurotoxin, but combined effects of them have not been reported. The present work aimed to reveal the effect of combined administration of *D*-gal and Al in mice and compare the effect of *D*-gal treatment with that of Al treatment. **Methods** Al was intragastrically administered and *D*-gal was subcutaneously injected into Kunming mice for 10 consecutive weeks. Learning and memory, cholinergic systems, as well as protein levels of amyloid β (Aβ) and hyperphosphorylated tau were determined using Morri water maze test, biochemical assays and immunohistochemical staining, respectively. **Results** The mice with combined treatment had obvious learning and memory deficits, and showed decreases in brain acetylcholine (ACh) level and in activities of choline acetyltransferase (ChAT) and acetylcholinesterase (AChE). Formation of senile plaque (SP)-like and neurofibrillary tangle (NFT)-like structures was also observed. The behavioral and pathological changes persisted for at least 6 weeks after withdrawal of *D*-gal and Al. **Conclusion** Combined use of *D*-gal and Al is an effective way to establish the non-transgenic Alzheimer's disease (AD) animal model, and is useful for studies of AD pathogenesis and therapeutic evaluation.

Keywords: Alzheimer's disease; brain change; *D*-galactose; aluminum; neurodegenerative disease; animal model

1 Introduction

Alzheimer's disease (AD) is a neurodegenerative disease with cognitive and memory dysfunctions. The main pathological features of AD are the formations of senile plaques (SPs) and neurofibrillary tangles (NFTs), as well as loss of cholinergic neurons in the basal forebrain[1]. The pathogenesis of AD is complex and remains still elusive. Genetic determinants have been defined by research on familial AD, which resulted in identification of mutations in 3 genes, amyloid β-protein precursor (APP) gene, presenilin-1 (PS1) gene, and presenilin-2 (PS2) gene[2]. However, in sporadic AD, the most common type of the disease, no mutations have been found. Therefore, transgenic AD animal models cannot faithfully model all aspects of AD[3-5]. The aim of the present study was to find a non-transgenic animal model that is relevant to the pathogenesis of AD.

It is known that *D*-galactose (*D*-gal) can mimic natural aging in mice. Following administration of *D*-gal, the

*These authors contributed equally to this work.
Corresponding author: Huan-Min LUO
Tel: +86-20-85220500; Fax: +86-20-85220160
E-mail: tlhm@jnu.edu.cn
Article ID: 1673-7067(2011)03-0143-13
Received date: 2010-07-05; Accepted date: 2011-03-28

malondialchehyche (MDA) level is increased while levels of antioxidant enzymes such as superoxide dismutase (SOD) are decreased in serum. The number of terminal deoxynucleotidyl transferase-mediated dUTP nick end labeling (TUNEL)-positive cells is significantly increased in the dentate gyrus (DG), as well as in CA1 and CA3 regions of the hippocampus. Besides, the bromodeoxyuridine (BrdU)-labeled proliferating cells and surviving cells in the DG are decreased significantly in number[6,7]. In addition, *D*-gal can induce behavioral impairment in C57BL/6J mice. *D*-gal-treated mice show a significantly longer escape latency in the Morris water maze test. In object recognition test, *D*-gal reduces the discriminatory ability of mice and also their locomotor activity[8]. Besides, *D*-gal can shorten the lifespan of fruit fly (*Drosophila melanogaster*) and housefly (*Musca domestica*), associated with an increase in oxidative stress[9]. *D*-gal treatment can accelerate mouse aging due to the formation of advanced glycation endproducts (AGEs). These changes may contribute to aging and induce early aging-related diseases[10,11].

Aluminum (Al) is a neurotoxin. After intragastric administration of Al, xanthine oxidase (XO) and glutathione peroxidase (GPX) activities are enhanced and depressed, respectively, leading to accumulation of intermediate toxic compounds such as hydrogen peroxide and hydroxyl radicals, which may mediate Al toxicity[12]. Following intracerebroventricular Al injection, immunoreactivity of astrocytes and phagocytic microglia, estimated by detection of glial fibrillary acidic protein (GFAP) and ED1, respectively, showed a stronger inflammatory response in rat brain. Enhancement of inflammation and interference with cholinergic projections may underlie the Al-caused learning and memory deficits[13]. Al has a specific toxic potential for cytoskeletal structures of brain cells[14]. The neuronal-specific markers microtubule-associated protein type 2 (MAP2) and neurofilament light subunit (NF68KD) are inhibited at lower Al concentrations (IC_{50} 180–630 μmol/L) than GFAP (IC_{50} 700–1 000 μmol/L), demonstrating that neurons have a particularly high sensitivity to Al in comparison to astrocytes[15]. Chronic exposure to Al reduces the basal activity of guanylate cyclase and impairs the glutamate-nitric oxide-cyclic guanosine monophosphate (cGMP) pathway *in vivo* and *in vitro*. Al reduces the cerebellar content of calmodulin and nitric oxide synthase by 34% and 15%, respectively. In Al-treated rats, the basal activity of soluble guanylate cyclase decreases by 66%, whereas the basal cGMP in cerebellar extracellular space decreases by 50%[16,17].

Although both *D*-gal and Al have neurotoxic effects, their combined neurotoxicity has not been explored. *D*-gal can mimic natural aging in mice and Al can induce the overexpression of APP in neurons, which may increase Aβ production. Thus, it is speculated that combined administration of *D*-gal and Al may yield pathological changes that model AD symptoms, including modifications of memory and cholinergic systems, as well as formation of SP and NFT. Based on the previous findings that combined use of *D*-gal and $AlCl_3$ can induce learning and memory impairment[18,19], the present work sought to provide an optimized mouse model for studying AD pathogenesis and drug evaluation, and to compare the effect of *D*-gal treatment with that of $AlCl_3$ treatment in mice.

2 Materials and methods

2.1 Animals A total of 192 female Kunming mice (2-month-old, 18–22 g body weight) were provided by Experimental Animal Center of Guangdong Province (qualified certificate number: 2008A022). Animals were housed under standard temperature (24±1) °C and diurnal conditions (lights on: 08:00–20:00), with access to food and water *ad libitum*.

2.2 Animal grouping and drug treatment *D*-gal (AMERSCO Co., Solon, OH, USA) was dissolved in normal saline and injected subcutaneously (0.12 mg/g, once per day). $AlCl_3$ (Guangzhou Chemical Reagent Factory, Guangzhou, China) was dissolved in double distilled water (DDW) and administered intragastrically (0.02 mg/g, once per day). The animals were randomly divided into 4 groups: control group, Al group, *D*-gal group and *D*-gal + Al group (n = 48 in each group). Each group was further randomly divided into 3 subgroups (n = 16 in each subgroup), of which one subgroup was treated for 8 weeks

and the other 2 subgroups were treated for 10 weeks (one tested at the end of the 10-week-period, and another tested 6 weeks later). Control groups received equal volumes of NS and DDW.

2.3 Learning and memory testing Morris water maze was used to assess the neurocognitive function at the end of 8-week-period, 10-week-period or 16-week-period. The Morris water maze was a circular pool, 100 cm in diameter and 50 cm in height, and was divided into 4 quadrants: east (E), south (S), west (W) and north (N). A transparent plastic escape platform, 29 cm high and 9 cm in diameter, was placed at the center of one of the 4 quadrants. The pool was filled with tap water to a depth of 30 cm, 1 cm above the platform. Water temperature was maintained at (24±1) ºC. The mice were trained with 4 trials per block, 2 blocks per day for 5 d. For each trial, the mouse was placed facing the wall at one of the 4 designated start points (E, S, W, and N). The mouse was then allowed 60 s to locate the platform. If it could not reach the platform within 60 s, it was gently guided to the platform and escape latency (the time taken to find the platform) was recorded as 60 s. The mouse was allowed to stay on the platform for 20 s until the next trial. For each block, a different start point was used in each trial. During each trial, the escape latency was automatically recorded using an overhead video camera-based DigBehv 3.0 system (Jiliang Software Technology Co. Ltd., Shanghai, China).

After completion of the 5-d trials, a spatial probe trial was performed. The platform was removed from the pool and the mouse was allowed to search it for 90 s. The time spent in the platform quadrant was measured and estimated as the percentage to total time spent in the pool.

2.4 The change of cholinergic system in mice brain After the completion of 5-d trials, acetylcholine (ACh) content was quantitatively measured using ACh ELISA kit (Uscn Life Science Inc., Wuhan, China). Choline acetyltransferase (ChAT) and acetylcholinesterase (AChE) activities were analyzed with the commercial kits (Nanjing Jiancheng Institute of Biotechnology, Nanjing, China), according to the standard spectrophotometric procedures.

2.5 SP immunohistochemical staining and NFT histochemical staining Mice were anesthetized by intraperitoneal injection of 3% pentobarbitone (0.01 mL/g), and then fixed by 4% paraformaldehyde solution (pH 7.4). Brain was removed and embedded in paraffin wax. Serial coronal sections were cut in 7-μm thickness and underwent conventional hematoxylin eosin (HE) staining, Aβ immunohistochemistry and Bielschowsky's silver staining, respectively, as described previously[20], using mouse anti-$A\beta_{1-42}$ antibody (Santa Cruz Biotech Co., MA, USA), mouse anti-$A\beta_{1-40}$ antibody (Wuhan Boster Biotech Co., China) and SABC immunohistochemical kit (Wuhan Boster Biotech Co., China)

2.6 Statistical analysis Data were expressed as mean±SD and analyzed with repeated one-way analysis of variance (ANOVA) using SPSS 11.0 statistical software (SPSS Inc., Chicago, IL, USA). $P < 0.05$ was considered as statistically significant.

3 Results

3.1 Morris water maze test As illustrated in Fig. 1, the combined administration of *D*-gal and Al for 8 and 10 weeks increased significantly the escape latency ($P < 0.01$), and this effect was maintained for at least 6 weeks ($P < 0.01$). Administration of Al alone for 8 weeks did not increase the escape latency, while treatment for 10 weeks showed a significant effect ($P < 0.01$), but this effect was not observed at the end of the 6-week-period of drug withdrawal. On the contrary, administration of *D*-gal alone for 8 and 10 weeks both increased the escape latency ($P < 0.05$ and $P < 0.01$, respectively), and this effect was still observed at the end of the 6-week-period of drug withdrawal ($P < 0.01$) (Fig. 1A).

The joint administration of *D*-gal and Al for 10 weeks significantly decreased the probing time spent in the target quadrant ($P < 0.01$), an effect persisting for 6 weeks ($P < 0.01$). Administration of Al alone for 10 weeks decreased the probing time ($P < 0.05$), but this effect disappeared at the end of the 6-week-period of drug withdrawal. On the contrary, administration of *D*-gal alone for 10 weeks decreased the probing time ($P < 0.05$), and this effect could also be detected at the end of the 6-week-period of drug withdrawal ($P < 0.05$) (Fig. 1B).

3.2 ACh content and activities of ChAT and AChE As

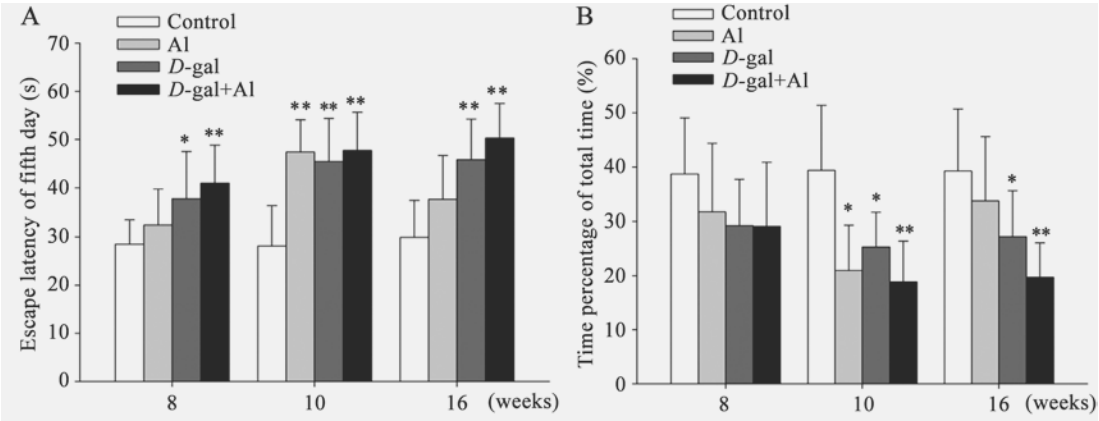

Fig. 1 The average of escape latency on the last day of training (day 5) (A) and the percentage of time spent in the target quadrant in the probe test (B) (n = 16 in each group). $^{*}P < 0.05$, $^{**}P < 0.01$ ***vs* the control group.**

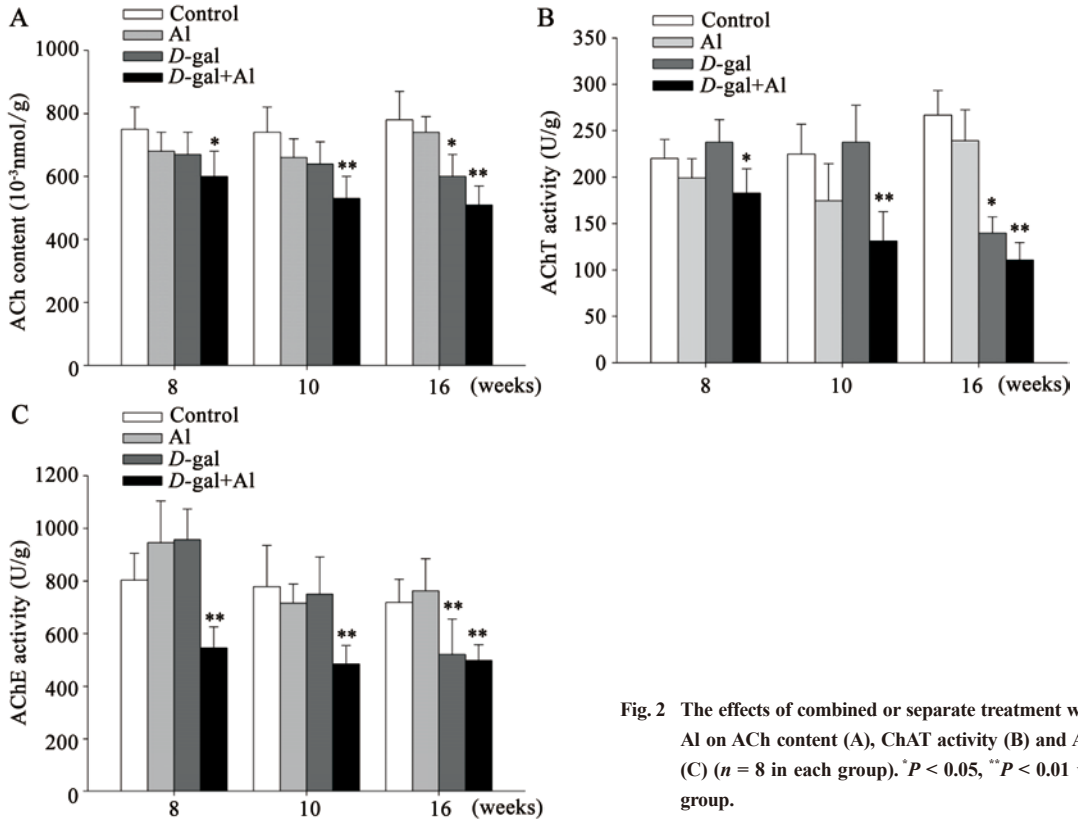

Fig. 2 The effects of combined or separate treatment with *D*-gal and Al on ACh content (A), ChAT activity (B) and AChE activity (C) (n = 8 in each group). $^{*}P < 0.05$, $^{**}P < 0.01$ ***vs* the control group.**

shown in Fig. 2, combined administration of *D*-gal and Al for 8 and 10 weeks significantly decreased ACh brain content ($P < 0.05$, $P < 0.01$, respectively), and this was also observed at the end of the 6-week-drug withdrawal ($P < 0.01$). In contrast, administration of Al alone had no effect. Administration of *D*-gal alone for 8 and 10 weeks both showed a trend of decrease in ACh content, but with no statistical significance. However, at the end of the 6-week-*D*-gal withdrawal (16 weeks in total), ACh content was significantly decreased ($P < 0.05$) (Fig. 2A).

Combined administration of *D*-gal and Al for 8 and 10 weeks both significantly decreased ChAT activity ($P < 0.05$,

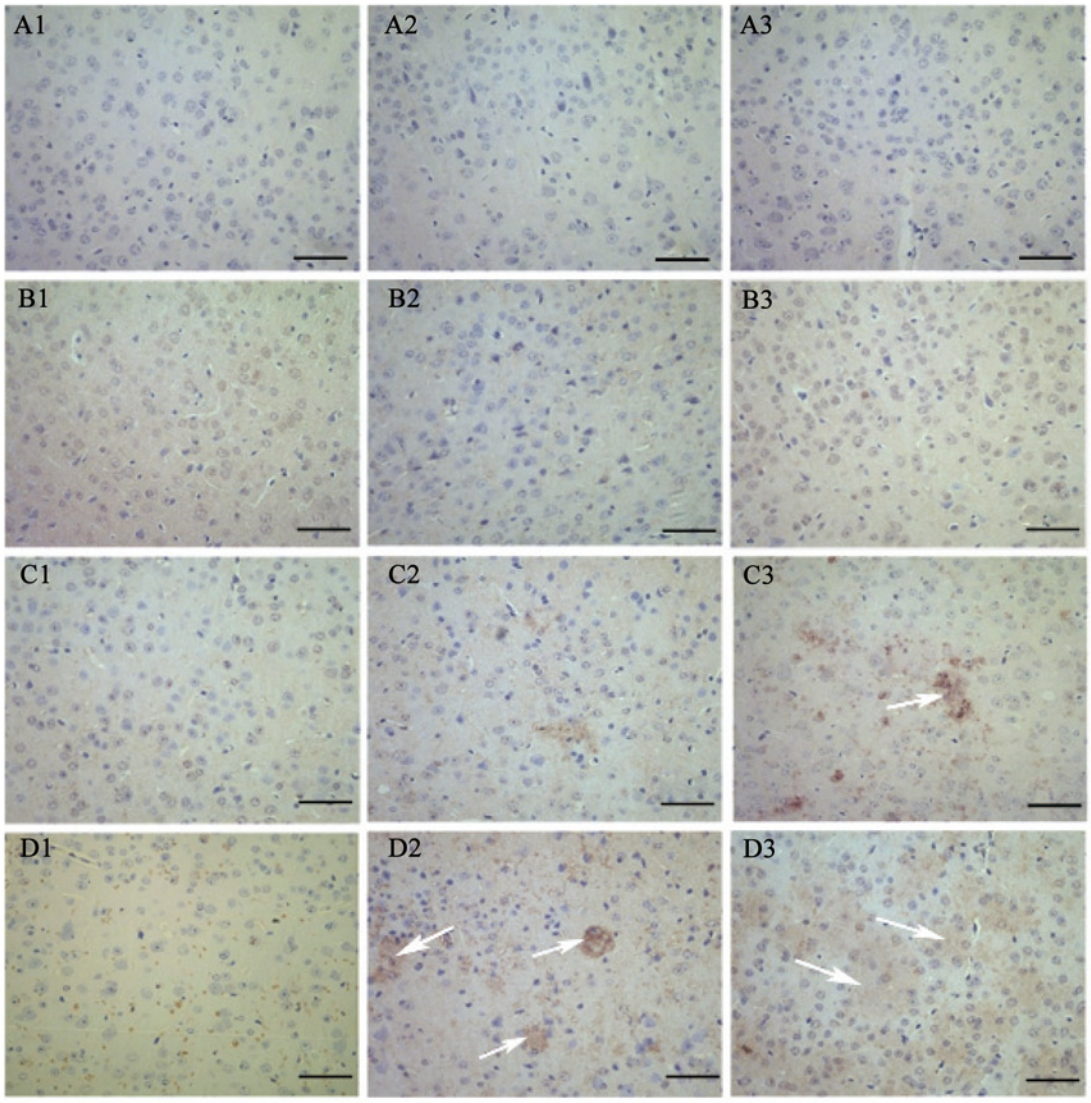

Fig. 3 Effects of Al (B), *D*-gal (C) or *D*-gal+Al (D) treatment for 8 weeks (A1–D1), 10 weeks (A2–D2), or 10 weeks plus 6 weeks of drug withdrawal (A3–D3), on $A\beta_{1-40}$ expression in mouse cortex. Arrows indicate products of $A\beta_{1-40}$ immunoreactive profiles, which is one of the central elements of senile plaque (SP). Many SP-like structures were present in the combined treatment group at week 10 (D2) and week 16 (D3). They were not found in control (A) or single treatment groups (B, C) except at week 16 in *D*-gal group (C3). Scale bar: 50 μm.

$P < 0.01$, respectively), which was still observed at the end of the 6-week-drug withdrawal ($P < 0.01$). However, neither Al nor *D*-gal significantly affected ChAT activity-when administered for 8 or 10 weeks. Six weeks after *D*-gal withdrawal (16 weeks in total), ChAT activity was suppressed slightly ($P < 0.05$) (Fig. 2B).

Similar as ChAT, AChE activity was significantly decreased by combined treatment with *D*-gal and Al for 8 and 10 weeks ($P < 0.01$), which persisted for 6 weeks ($P < 0.01$), whereas administration of Al alone had no effect. *D*-gal treatment alone for 8 or 10 weeks did not decrease AChE activity, either, but at the end of the 6-week-period of drug withdrawal, AChE activity was detected to be slightly decreased ($P < 0.05$) (Fig. 2C).

3.3 $A\beta_{1-40}$ and $A\beta_{1-42}$ immunohistochemistry and NFT histochemical staining At the end of the experiment, some mice harbored signs of premature aging, such as kyphosis and hypotrichosis. HE staining did not show any

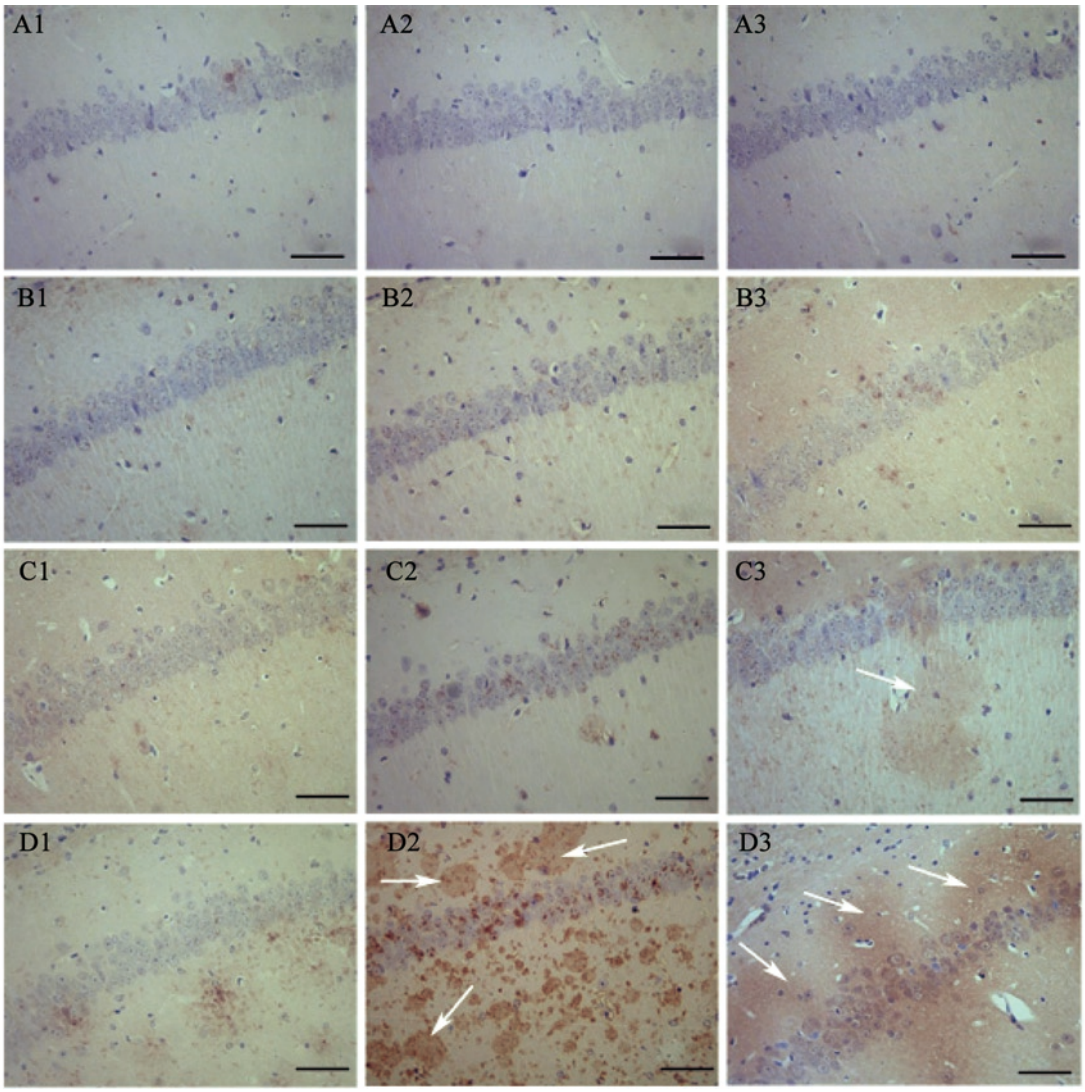

Fig. 4 Effects of Al (B), *D*-gal (C) or *D*-gal+Al (D) treatment for 8 weeks (A1–D1), 10 weeks (A2–D2), or 10 weeks plus 6 weeks of drug withdrawal (A3–D3), on $A\beta_{1\text{-}40}$ expression in the hippocampus. Arrows indicate the $A\beta_{1\text{-}40}$ immunoreactive profiles. Many SP-like structures were present in the combined treatment group at week 10 (D2) and week 16 (D3). However, they were not found in control (A) or single treatment groups (B, C), except at week 16 in *D*-gal group. Scale bar: 50 μm.

pathological differences among the treated and control animals. No $A\beta_{1\text{-}40}$ or $A\beta_{1\text{-}42}$ immunoreactivity was detected in control mice, showing that $A\beta_{1\text{-}40}$ was not or minimally expressed in those mice. By contrast, $A\beta_{1\text{-}40}$ (Figs. 3, 4) and $A\beta_{1\text{-}42}$ (Figs. 5, 6) immunoreactivity was detected in the mice subjected to combined *D*-gal and Al treatment. Aβ accumulated and formed SPs in hippocampus and cortex, and in the vicinity, some deformed swelled neurons were present. Besides, some β-amyloid protein-like immunoreactive (APLI) neurons were observed, in which the reaction product was distributed in neuronal processes and around nuclei. Bielschowsky silver staining (Figs. 7, 8) revealed the presence of NFT and SP-positive neurons in the combined treatment but not the control group, confirming the $A\beta_{1\text{-}40}$ immunohistochemical results.

4 Discussion

Brain toxicity following *D*-gal treatment for a long pe-

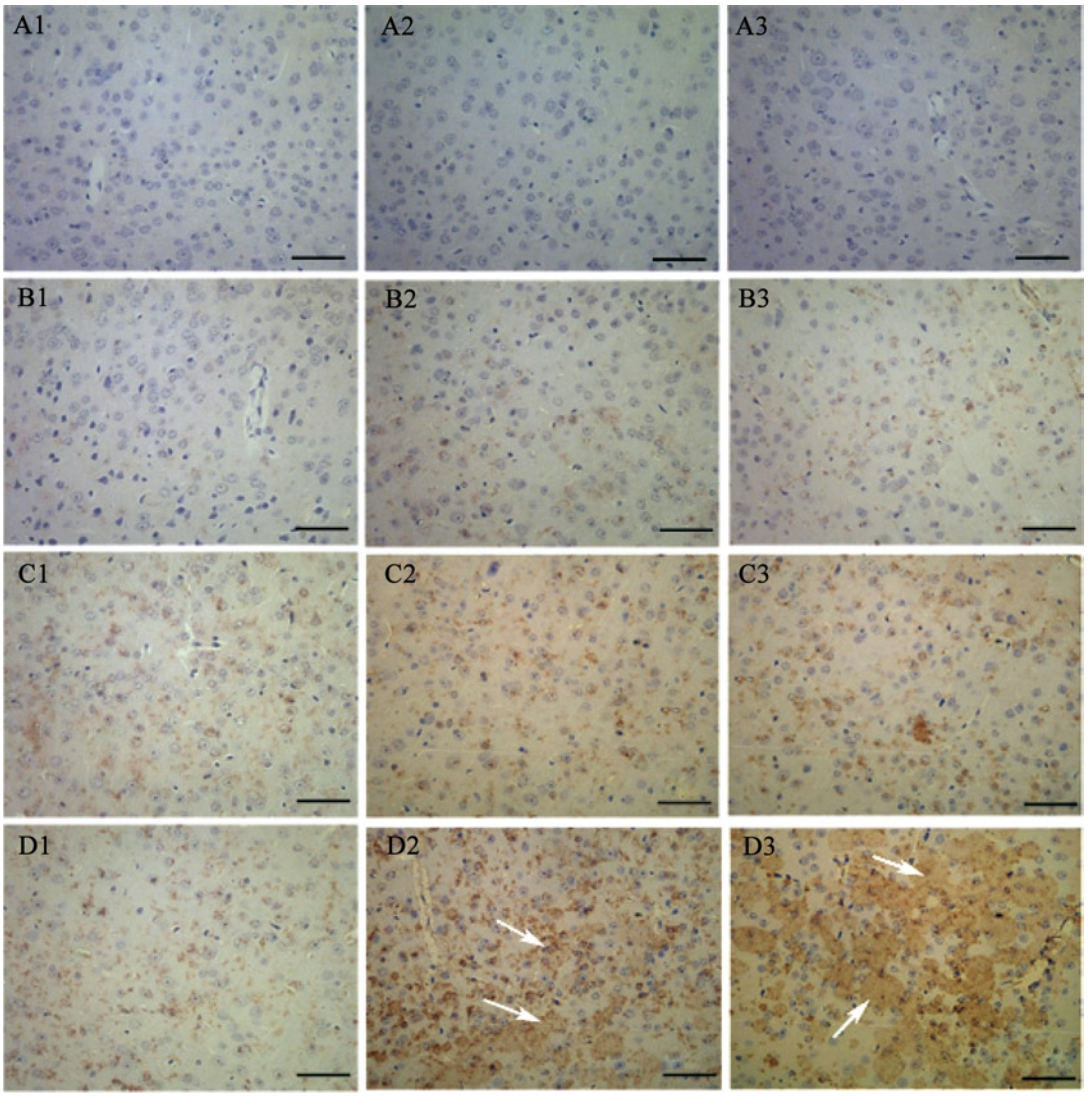

Fig. 5 Effects of Al (B), *D*-gal (C) or *D*-gal+Al (D) treatment for 8 weeks (A1–D1), 10 weeks (A2–D2) or 10 weeks plus 6 weeks of drug withdrawal (A3–D3), on the expression of $A\beta_{1-42}$ in the cortex. Arrows indicate $A\beta_{1-42}$ immunoreactive profiles. $A\beta_{1-42}$ was one of the central elements of SP. Many SP-like structures were present in the combined treatment group at week 10 (D2) and week 16 (D3). They were not found in control (A) or single treatment groups (B, C). Scale bar: 50 μm.

riod in young adult mice can be attributed to its metabolite, *D*-gal ethanol, which cannot be metabolized further and accumulates inside cells. This may result in increased osmotic pressure, thereby inducing cell swelling and metabolic dysfunction. *D*-gal may also lead to formation of AGEs *in vivo*, which may accelerate the aging process. *D*-gal-treated mice display significant increases in memory latency time and error rate in behavioral tests, and increased skin hydroxyproline content[11]. Furthermore, these mice show significant decreases in motor activity, lymphocyte mitogenesis, interleukin-2 (IL-2) production, and SOD enzyme activity. The level of reactive oxygen species increases *in vivo* and cell membrane lipids are damaged, resulting in multiple organ and system disorders. These pathological alterations induced by *D*-gal resemble natural aging. In the present experiment, Kunming mice treated with *D*-gal (0.12 mg/g) for 10 weeks provided a model of aging that mimicked some features of AD. Some mice harbored signs

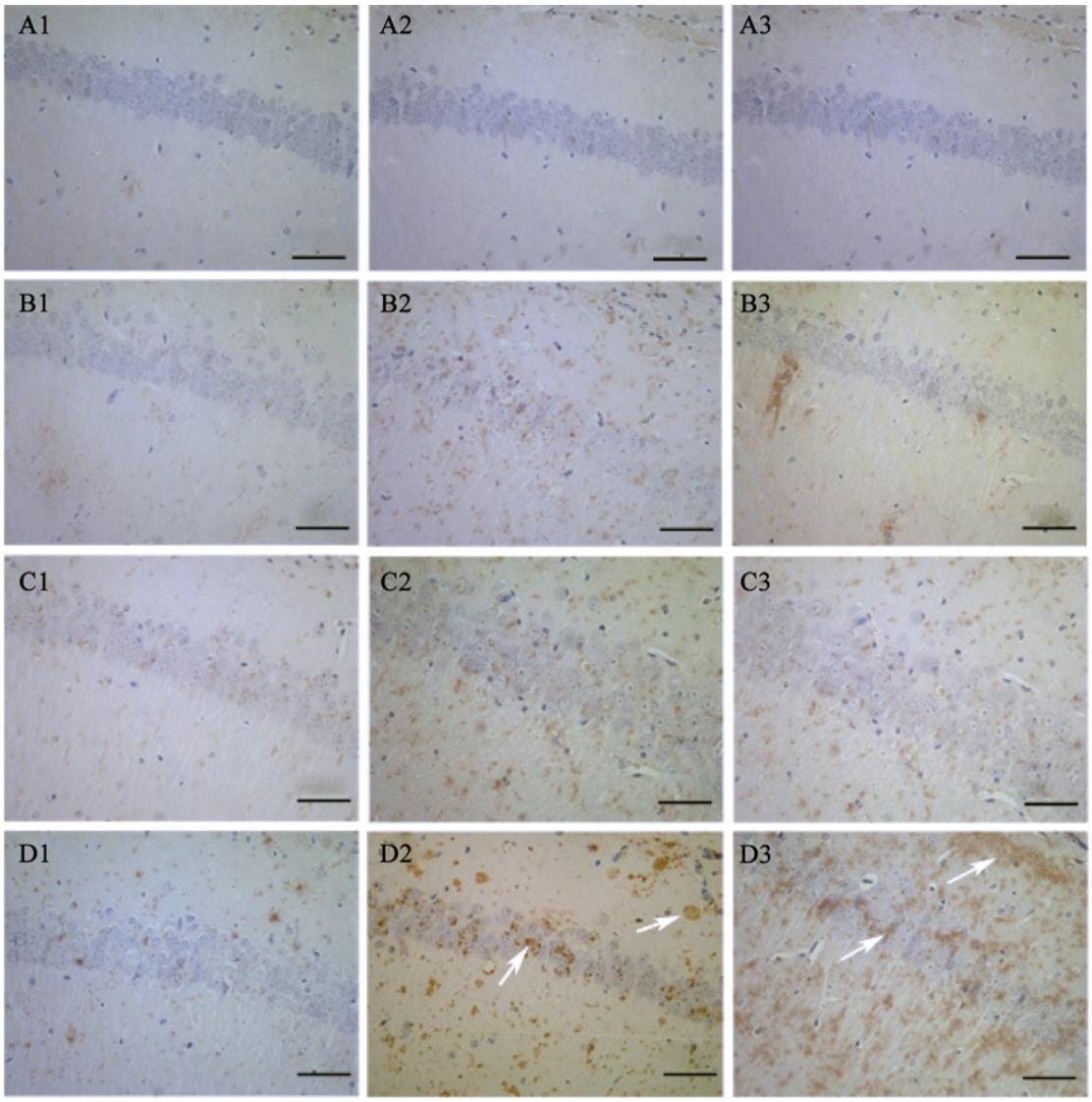

Fig. 6 Effects of Al (B), *D*-gal (C) or *D*-gal+Al (D) treatment for 8 weeks (A1–D1), 10 weeks (A2–D2), or 10 weeks plus 6 weeks of drug withdrawal (A3–D3), on the expression of $A\beta_{1\text{-}42}$ in the hippocampus. Arrows indicate $A\beta_{1\text{-}42}$ immunoreactive profiles. Many SP-like structures were present in the combined treatment group at week 10 (D2) and week 16 (D3). They were not found in control (A) or single treatment groups (B, C). Scale bar: 50 μm.

of premature aging such as humpback, hair loss and slow locomotion from approximately 60 d of treatment.

Previous research showed that AD brains contain increased levels of Al. Atom absorption spectrography revealed that Al content is (3.6±2.9) mg/g dry weight in AD brain, higher than the content (1.8±0.8) mg/g in normal human brain. Brain cell degeneration can be produced when Al level is above 4 mg/g[21,22]. Free Al may enter the brain via olfactory nerves and by crossing the blood-brain barrier. Al can replace calcium and magnesium, binding to glutamic acid and arginine in the amino acid chain, which yields to the formation of stable compound of Al-glutamate or Al-arginine that precipitates in the cerebral cortex, hippocampus and amygdala where glutamatergic neurons are abundant. Al binds transferrin in the plasma. Abundant transferrin receptors exist in cerebral cortex, hippocampus,

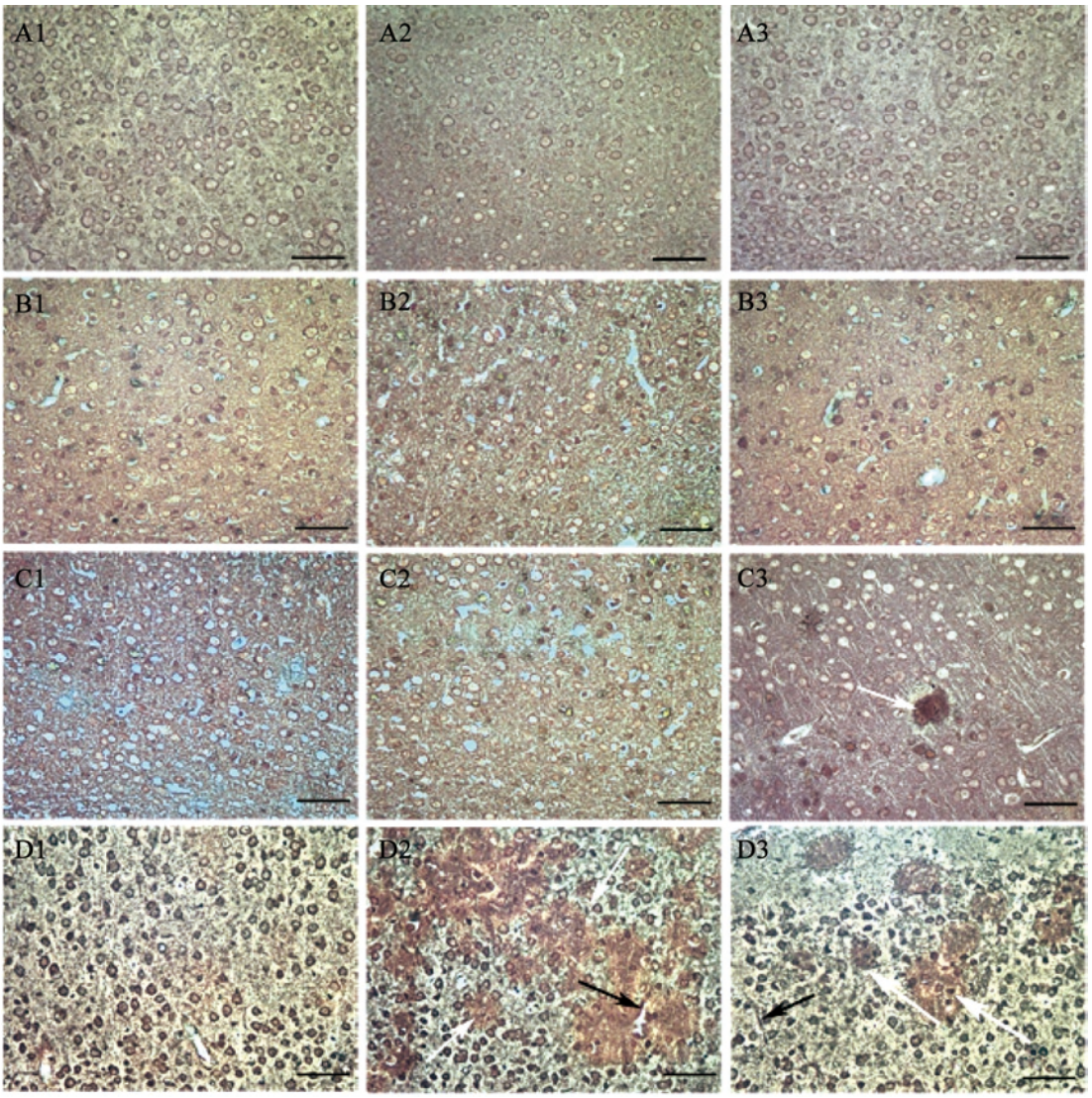

Fig. 7 Bielshovsky silver staining showed the effects of Al (B), *D*-gal (C), *D*-gal+Al (D) treatment for 8 weeks (A1–D1), 10 weeks (A2–D2), or 10 weeks plus 6 weeks of drug withdrawal (A3–D3) on the numbers of SP-like and NFT-like structures in the cortex. White arrows indicate the round SP-like structures outside the cells, while black arrows indicate filamentous NFT-like structures inside cells. Many SP-like and NFT-like structures were present in combined treatment groups at week 10 (D2) and week 16 (D3), but not in control (A) or single factor-treated groups (B, C). Scale bar: 50 μm.

septal nuclei and amygdala, where Al is prone to form deposits[23,24]. Al toxicity is more readily induced in adult and aged than in juvenile animals, and susceptibility to the behavioral toxicity of Al increases steadily with age[25]. Following Al lactate or tartrate subcutaneous injection for 30 d in rabbits, formations of intraneuronal NFTs are detected in brain stem, cerebral cortex and hippocampus[14]. It has also been reported that Al increases *APP* gene expression in the brain[26]. Administration of aluminum trichloride in rats for 3 months induces APLI neurons in all sectors of the dorsal hippocampal formation[27]. Although SPs were not found, this study indicated that Al can increase Aβ generation in neurons. Finally, metal chelating agent with trivalence has been suggested to slow the progress of AD[28]. This set of data strongly indicates that Al plays a significant role in AD.

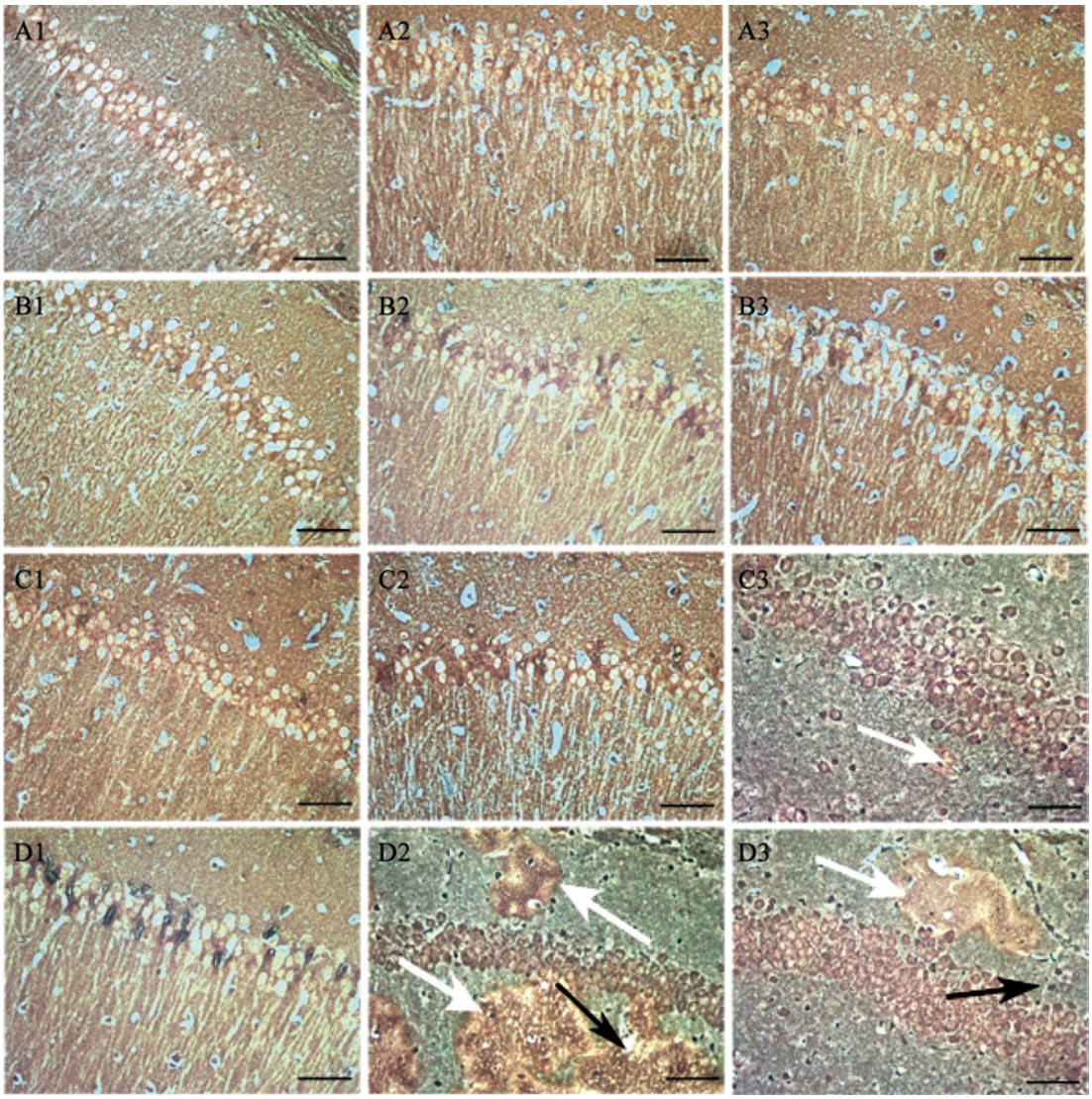

Fig. 8 Bielshovsky silver staining showed the effects of Al (B), *D*-gal (C), *D*-gal+Al (D) treatment for 8 weeks (A1–D1), 10 weeks (A2–D2), or 10 weeks plus 6 weeks of drug withdrawal (A3–D3) on the numbers of SP-like and NFT-like structures in the cortex. White arrows indicate the round SP-like structures outside the cells, while black arrows indicate filamentous NFT-like structures inside cells. Many SP-like and NFT-like structures were present in combined treatment group at week 10 (D2) and week 16 (D3), but not in control (A) or single factor-treated groups (B, C). Scale bar: 50 μm.

Our experiments showed that combined use of *D*-gal and Al resulted in declines in learning and memory ability and dysfunction of cholinergic neurons, which appeared earlier, being more severe and more persistent than those induced by single administration of *D*-gal or Al. ACh is an important neurotransmitter implicated in learning and memory. The content of ACh is positively correlated with learning and memory, and can be increased in hippocampus and cortex by animal training[29]. ACh is synthesized by ChAT, and degraded by AChE, both of which have reduced activity in AD brain, resulting in an overall decrease of ACh concentration that may contribute to the decline in learning and memory. However, reports on the change of AChE activity in AD animal models are not consistent, with some reporting decreased, and others reporting increased concentration. These discrepancies may be due to

the differences in animal models and experimental methods, including sampling time. Our results showed that brain ACh content, as well as ChAT and AChE activities, decreased in our AD model ($P < 0.01$), suggesting that cholinergic dysfunction may be the cause of the observed deficits in spatial memory in the Morris water maze test. One interest of our model lies in its replication of cholinergic defects in AD.

Comparative analysis of 3 kinds of animal models showed that Al alone did not produce learning dysfunction at week 16 or cholinergic dysfunctions at week 10 or 16 (Table 1). On the contrary, *D*-gal was sufficient to impair learning, and the effects were still observed at the end of 6-week drug withdrawal following 10-week administration. Besides, *D*-gal treatment alone for 10 weeks plus 6-week-drug withdrawal was sufficient to produce cholinergic dysfunctions in mice, which in some regards can be considered as the experimental contribution as it is corresponding to the lasting effects in this model. Taken together, the learning and cholinergic dysfunctions of combined model mostly depend on the *D*-gal effect.

Both $A\beta_{1\text{-}40}$ and $A\beta_{1\text{-}42}$ immunohistochemical staining showed that Aβ was overexpressed in *D*-gal + Al model. Excessive Aβ accumulated and deposited in SP-like structures containing degenerated neurons and debris. In the Al model, APLI neurons were present, but no SPs were observed. Mice treated with *D*-gal alone showed no or few APLI neurons. Both SP and NFT can be observed by silver staining. Silver staining showed that many SP-like or NFT-like structures were present in *D*-gal+Al group, while no or very few SP-like or NFT-like structures were detected in *D*-gal or Al group. These results are consistent with the Aβ immunohistochemical results, indicating that the addition of Al to *D*-gal can increase the NFT and plaque loads, and produce neuronal loss. The mechanism underlying SP-like structure increase might be related to APP overexpression induced by Al, followed by Aβ overproduction. SP-like and NFT-like structures may damage normal brain structure, thereby potentially contributing to learning and memory impairment, which result in more serious learning and memory dysfunction in combined use of *D*-gal and Al than use of them respectively.

In conclusion, the mice receiving combined administration of *D*-gal and Al exhibit many features of AD such as learning and memory impairment, decreases of ACh content, ChAT and AChE deficiencies, accumulation of Aβ in neuron, and the formation of SP and NFT. The Alzheimer-like brain lesions can be maintained for at least 6 weeks. The present mouse model established by combined administration of *D*-gal and Al provides an effective, simple and inexpensive non-transgenic AD animal model for research

Table 1. The comparison of 3 kinds of animal models

Test content	Al			*D*-gal			*D*-gal+Al		
	8 weeks	10 weeks	16 weeks*	8 weeks	10 weeks	16 weeks*	8 weeks	10 weeks	16 weeks*
Learning and memory									
Escape latency	–	+	–	+	+	+	++	++	++
Time Percentage	–	+	–	–	+	+	–	++	++
Cholinergic system									
ACh content	–	–	–	–	–	+	+	++	++
ChAT activity	–	–	–	–	–	+	+	++	++
AChE activity	–	–	–	–	–	+	+	++	++
Brain pathology									
Neuronal loss	–	–	–	–	–	–	±	+	+
SP	–	–	±	–	–	±	+	++	++
NFT	–	–	±	–	–	±	+	++	++

–: negative change, +: positive change, ++: more serious positive change; ±: uncertainty; *: treatment for 10 weeks plus 6 weeks of drug withdrawal.

ACh: acetylcholine. ChAT: choline acetyltransferase. AChE: acetylcholinesterase. SP: senile plaque. NFT: neurofibrillary tangle.

on AD pathogenesis and for drug evaluation.

Acknowledgements: This work was supported by National Natural Science Foundation of China (No. 30271502). We are grateful to Wen WENG and Pei-Fen ZHANG for technical assistance.

References:

[1] Whitehouse PJ, Price DL, Struble RG, Clark AW, Coyle JT, Delon MR. Alzheimer's disease and senile dementia: loss of neurons in the basal forebrain. Science 1982, 215(4537): 1237–1239.

[2] Selkoe, DJ. Alzheimer's disease: Genes, proteins, and therapy. Physiological Rev 2001, 81(2): 741–766.

[3] Duff K, Hardy J. Alzheimer's disease: mouse model made. Nature 1995, 373(6514): 476–477.

[4] Kawabata S, Higgins GA, Gordon JW. Amyloid plaques, neurofibrillary tangles and neuronal loss in brains of transgenic mice overexpressing a C-terminal fragment of human amyloid precursor protein. Nature 1991, 354(6353): 476–478.

[5] Quon D, Wang Y, Catalano R, Scardina JM, Murakami K, Cordell B. Formation of beta-amyloid protein deposits in brains of transgenic mice. Nature 1991, 352(6332): 239–241.

[6] Ho SC, Liu JH, Wu RY. Establishment of the mimetic aging effect in mice caused by *D*-galactose. Biogerontology 2003, 4(1): 15–18.

[7] Zhang Q, Li X, Cui X, Zuo P. *D*-galactose injured neurogenesis in the hippocampus of adult mice. Neurol Res 2005, 27(5): 552–556.

[8] Wei H, Li L, Song Q, Ai H, Chu J, Li W. Behavioural study of the *D*-galactose induced aging model in C57BL/6J mice. Behav Brain Res 2005, 57(2): 245–251.

[9] Cui X, Wang L, Zuo P, Han Z, Fang Z, Li W, *et al. D*-galactose-caused life shortening in *Drosophila melanogaster* and *Musca domestica* is associated with oxidative stress. Biogerontology 2004, 5(5): 317–325.

[10] Ida H, Ishibashi K, Reiser K, Hjelmeland LM, Handa JT. Ultrastructural aging of the RPE-Bruch's membrane-choriocapillaris complex in the *D*-galactose-treated mouse. Invest Ophthalmol Vis Sci 2004, 45(7): 2348–2354.

[11] Song X, Bao M, Li D, Li YM. Advanced glycation in *D*-galactose-induced mouse aging model. Mech Ageing Dev 1999, 108(3): 239–251.

[12] Moumen R, Ait-Oukhatar N, Bureau F, Fleury C, Bouglé D, Arhan P, *et al.* Aluminium increases xanthine oxidase activity and disturbs antioxidant status in the rat. J Trace Elem Med Biol 2001, 15(2-3): 89–93.

[13] Platt B, Fiddler G, Riedel G, Henderson Z. Aluminium toxicity in the rat brain: histochemical and immunocytochemical evidence. Brain Res Bull 2001, 55(2): 257–267.

[14] Boni UD, Otvos A, Scott JW, Crapper DR. Neurofibrillary degeneration induced by systemic aluminum. Acta Neuropathol (Berl) 1976, 35(4): 285–294.

[15] Muller JP, Bruinink A. Neurotoxic effects of aluminium on embryonic chick brain cultures. Acta Neuropathol (Berl) 1994, 88(4): 359–366.

[16] Hermenegildo C, Saez R, Minoia C, Manzo L, Felipo V. Chronic exposure to aluminium impairs the glutamate-nitric oxide-cyclic GMP pathway in the rat *in vivo*. Neurochem Int 1999, 34(3): 245–253.

[17] Henderson AS. Epidemiology of dementia disorders. In: Wurtman RJ, Corkin S, Growdon JH, Ritter-Walker E (Eds). Alzheimer's disease. Vol. 51 Advances in neurology. New York: Raven Press, 1990: 15–25.

[18] Luo HM, Xiao F. Alzheimer-like pathological changes of mice induced by D-galactose and aluminum trichloride. Chin J Pharmacol Toxicol 2004, 18(1): 22–26.

[19] Luo HM, Xiao F. Preparing method for Alzheimer disease animal model [P]. CN, CN1278603.2006-10-11.

[20] Litchfield S, Nagy Z. New temperature modification makes the Bielschowsky silver stain reproducible. Acta Neuropathologica 2001, 101(1): 17–21.

[21] Andrasi E, Pali N, Molnar Z, Kösel S. Brain aluminum, magnesium and phosphorus contents of control and Alzheimer-diseased patients. J Alzheimers Dis 2005, 7(4): 273–284.

[22] Fattoretti P, Bertoni-Freddari C, Balietti M, Giorgetti B, Solazzi M, Zatta P. Chronic aluminum administration to old rats results in increased levels of brain metalions and enlarged hippocampal mossy fibers. Ann N Y Acad Sci 2004, 1019(8): 44–47.

[23] Deloncle R, Guillard O. Mechanism of Alzheimer's disease: arguments for a neurotransmitter-aluminium complex implication. Neurochem Res 1990, 15 (12): 1239–1245.

[24] McLachlan DR, Lukiw WJ, Cho HJ, Carp RI, Wisniewski H. Chromatin structure in scrapie and Alzheimer's disease. Can J Neurol Sci 1986, 13 (4 Suppl): 427–431.

[25] Yokel RA. Aluminum produces age related behavioral toxicity in the rabbit. Neurotoxicol Teratol 1989, 11(3): 237–242.

[26] Guo GW, Wu YL, Yang XH, Guo LN, Yang YX. Effects of aluminum chloride on amyloid β-protein precursor and glial fibrillary acidic protein expression in rat cortex. Chin J Pharmacol Toxicol 1999, 13(3): 227–230.

[27] Qian YH, Yang J, Ren HM, Hu HT, Zhang ZJ. Immunocytochemical study of amyloid protein accumulation in dorsal hippocampal formation of a rat model of dementia. J Xian Medi Univ 1997, 18(3): 304–307.

[28] McLachlan DR, Kruck TP, Lukiw WJ, Krishnan SS. Would decreased aluminum ingestion reduce the incidence of Alzheimer's disease? CMAJ 1991, 145(7): 793–804.

[29] Pepeu G, Giovannini MG. Changes in acetylcholine extracellular levels during cognitive processes. Learn Mem 2004, 11(1): 21–27.

D- 半乳糖和铝联合应用诱导大脑产生阿尔茨海默病样损伤

肖飞[1], 李晓光[2,3], 张晓裕[1], 侯军代[1], 林炼峰[1], 高勤[2,3], 罗焕敏[1,2,3]

[1] 暨南大学医学院药理学系 , 广州 510632

[2] 暨南大学脑科学研究所 , 广州 510632

[3] 暨南大学 - 香港大学脑功能与健康联合实验室 , 广州 510632

摘要：目的 *D*-半乳糖能制作亚急性衰老模型，铝具有神经毒性，但两者联合应用的作用未见报道。本研究旨在探讨*D*-半乳糖和铝联合应用对动物学习记忆、脑内生化和病理的影响，以及与单独应用*D*-半乳糖或铝所制作的动物模型相比较。**方法** 昆明小鼠单独皮下注射*D*-半乳糖、单独灌胃铝以及既注射*D*-半乳糖又灌胃铝，制作动物模型, 共给药8周或10周, 10周后再停用药物6周。在第8、10、16周末，采用Morris水迷宫检测小鼠学习记忆能力, 生化学方法检测脑内乙酰胆碱能系统, 免疫组化法检测老年斑和神经原纤维缠结的形成。**结果** 联合应用*D*-半乳糖和铝后，小鼠表现出明显的学习和记忆力障碍，并且其脑内乙酰胆碱水平降低，乙酰胆碱转移酶和胆碱脂酶活性下降，出现老年斑样和神经原纤维缠结样病理改变。停止给药后，其行为学、生化和病理改变至少能维持6周以上。**结论** 小鼠中*D*-半乳糖和铝联合应用是一个有效的非转基因阿尔茨海默病(Alzheimer's disease, AD)模型，可用于AD病理研究和相关治疗药物的评价。

关键词：阿尔茨海默病；脑改变；*D*-半乳糖；铝；神经退行性疾病；动物模型